https://doi.org/10.5194/acp-2019-1142
Preprint. Discussion started: 26 February 2020


Atmospheric Chemistry and Physics Discussions

# Elucidating the pollution characteristics of nitrate, sulfate and ammonium in $PM_{2.5}$ in Chengdu, southwest China based on long-term observations

Liuwei Kong[1], Miao Feng[2], Yafei Liu[1], Yingying Zhang[1], Chen Zhang[1], Chenlu Li[1], Yu Qu[3], Junling An[3], Xingang Liu[1,*], Qinwen Tan[2,*], Nianliang Cheng[4], Yijun Deng[5], Ruixiao Zhai[5], Zheng Wang[5]

[1]State Key Laboratory of Water Environment Simulation, School of Environment, Beijing Normal University, Beijing 100875, China

[2]Chengdu Academy of Environmental Sciences, Chengdu 610072, China

[3]State Key Laboratory of Atmospheric Boundary Layer Physics and Atmospheric Chemistry, Institute of Atmospheric Physics, Chinese Academy of Sciences, Beijing 100029, China

[4]Beijing Municipal Environmental Monitoring Center, Beijing 100048, China

[5]Yuncheng Municipal Ecological Environment Bureau, Yuncheng, 044000, China

* Corresponding author.

E-mail addresses: liuxingang@bnu.edu.cn (Xingang Liu) and 11923345@qq.com (Qinwen Tan)

**Abstract**

Nitrate, sulfate and ammonium (NSA) are the main secondary inorganic aerosols of $PM_{2.5}$ and play an important role in the process of air pollution. However, few studies have analysed the variation characteristics of NSA in $PM_{2.5}$ and the effects of control measures through long-term observations. In this study, a long-term observational experiment was conducted from January 1, 2015 to December 31, 2017 in Chengdu, southwest China. NSA pollution characteristics, chemical conversion generation, emission reduction control sensitivity analysis and pollutant regional transport characteristics were analysed. The concentrations of sulfate and ammonium in $PM_{2.5}$ have been well reduced, but the effect of reducing nitrate was not obvious. Seasonal and diurnal variations have obvious characteristics, winter still has a high NSA concentration and emission intensity, and the concentration during the day was higher

https://doi.org/10.5194/acp-2019-1142
Preprint. Discussion started: 26 February 2020


Atmospheric Chemistry and Physics Discussions

than that at night. Although the workday concentration was slightly higher than the weekend concentration, the difference was nonsignificant. The chemical conversion characteristics of NSA formation were comprehensively analysed, and the aqueous phase oxidation process plays an important role in the conversion of NOx, $SO_2$ and $NH_3$ to NSA. The ammonia-rich environment became increasingly obvious in the atmosphere of Chengdu. Under these conditions, the sensitivity of NSA concentration variation was analyses using the ISORROPIA-II thermodynamic model, and the results show that by reducing NOx and $SO_2$ emissions, not only can reduce the nitrate and sulfate in $PM_{2.5}$, but also help reduce the formation of ammonium nitrate and ammonium sulfate to reduce ammonium. The results also show that while carrying out NSA emission reduction, it is also possible to generate potential risks of changes in aerosol pH. Combined with meteorological conditions and a potential source contribution function (PSCF) analysis, local emissions and regional emissions of pollutants are found to have important impacts on Chengdu's atmospheric environment. This research result not only provides an assessment of the current atmospheric emission reduction effect but also provides an important reference for determining methods to further reduce the NSA concentration in atmospheric $PM_{2.5}$.

**Keywords:** Secondary inorganic aerosols; Long-term observations; Pollution characteristics; Chemical conversions; Source analysis; Chengdu

## 1 Introduction

In recent years, with the rapid development of China's domestic economy and acceleration of the urbanization process, energy consumption and pollutant emissions have also increased, which increases the burden on the atmospheric environment, and severe air pollution has become the focus of social concern (Liu et al., 2013b;An et al., 2019;Fu et al., 2014;Zhao et al., 2017). When air pollution forms, $PM_{2.5}$ (aerodynamic diameter less than 2.5 μm) mass concentrations can reach a higher pollution level, which not only reduces atmospheric visibility but also carries a large number of toxic species into the human lungs, increasing the risks of cardiovascular and cerebrovascular

https://doi.org/10.5194/acp-2019-1142
Preprint. Discussion started: 26 February 2020


Atmospheric Chemistry and Physics Discussions

diseases, as well as harming human health (Chang et al., 2018;Tie et al., 2009;Kong et al., 2019;Zhao et al., 2018;Yang et al., 2015b). Nitrate, sulfate, ammonium, organic matter and elemental carbon are the main components of $PM_{2.5}$, among which sulfate, nitrate and ammonium (NSA) are the main secondary inorganic components in $PM_{2.5}$ (Ji et al., 2019;Zheng et al., 2016). NSA mainly originates from the secondary aerosols produced by complex chemical reactions of NOx, $SO_2$and $NH_3$ from coal combustion, vehicle exhaust emissions and agricultural sources (Liu et al., 2013a;Wang et al., 2016;Tian et al., 2017).

Because China's current main energy consumption is still fossil fuels, which are widely used in industry, vehicles and residentially, the emission reduction space of NSA is still restricted by a large number of gaseous precursors of NSA (Zhao et al., 2018;Tong et al., 2019). In addition, the chemical conversion of$NO_2$, $SO_2$ and $NH_3$ to form NSA is still very complex. For example, photochemistry may affect the formation of NSA at high solar radiation, and the homogeneous reaction may dominate the formation of NSA in high relative humidity (Cheng et al., 2016;Sun et al., 2014;Wang et al., 2016;Ohta and Okita, 1990). The formation of sulfate can increase the acidity of aerosols (Sun et al., 2014). In contrast, the presence of $NH_3$ can play a role in neutralization and maintain the acid-base balance of aerosols (Wang et al., 2016). If improper control measures are taken in pollution reduction control, such as further ammonia emission reduction, acidification of aerosols and environmental problems of acid rain are the likely result (Liu et al., 2019c). In addition to the local emission of pollutants, regional transport is also an important influencing factor. Determination of regional transport sources of pollutants, taking regional joint prevention and control measures, and jointly reducing the emissions of pollutants will enable better air control effects, particularly in the Beijing-Tianjin-Hebei region of northern China (Chen et al., 2019a).

The characteristics of higher concentrations proportion of nitrate, sulfate and ammonium in $PM_{2.5}$ were also found in other polluted areas in China, such as Beijing-Tianjin-Hebei, the Yangtze River Delta, the Pearl River Delta, the Fenwei Plain,

https://doi.org/10.5194/acp-2019-1142
Preprint. Discussion started: 26 February 2020


Atmospheric Chemistry and Physics Discussions

Chengdu-Chongqing region (An et al., 2019;Li et al., 2017;Liu et al., 2019d). In response to this situation, the Chinese government issued an Air Pollution Prevention and Control Action Plan (2013-207) in 2013 to reduce pollutant emissions and improve air quality (Ministry of Ecology and Environment of the People's Republic of China, 2013, last access: 12 February 2020). A large number of treatment measures have been taken in coal combustion, motor vehicle emissions and phase out of outdated industrial capacities, and by 2017, China's ambient air quality control measures have achieved good results (Liu et al., 2019a;Chen et al., 2019b;Cheng et al., 2019;Li et al., 2019b). In Beijing, $PM_{2.5}$, $NO_2$ and $SO_2$ decreased by 35.2%, 17.9% and 69.8%, respectively, in 2017 compared with 2013 (Beijing Municipal Ecology and Environment Bureau，2017, last access: 12 February 2020). In Chengdu, $PM_{2.5}$, $NO_2$ and $SO_2$ decreased by 42.3%, 15.9% and 64.5%, respectively, in 2017 compared with 2013 (Chengdu Municipal Ecology and Environment Bureau, 2017, last access: 12 February 2020). To continue to promote air quality improvement, the Chinese government launched the " Three-Year Action Plan for Winning the Blue Sky Defense Battle" in 2018, which puts forward stricter requirements on how to further promote the implementation of emission reduction plans (the Sate Council, 2018, last access: 12 February 2020). Through long-term observations, a comprehensive analysis of $PM_{2.5}$ chemical composition and source characteristics is carried out to verify the current implementation effects of emission reduction, and in-depth analyses of pollution reduction control characteristics is of great significance for the next step in air pollution control. However, observations with high time resolution are very rare, and the time period of these atmospheric observations usually includes several pollution processes or last for weeks or months; thus, it is difficult to analyse the long-term change characteristics of air pollution through comprehensive observational means (Sun et al., 2013;Tie et al., 2017;Guo et al., 2014). Especially in the Sichuan Basin of Southwest China, there are few long-term observational experiments on NSA, which is the main chemical component of $PM_{2.5}$.

https://doi.org/10.5194/acp-2019-1142
Preprint. Discussion started: 26 February 2020


Atmospheric Chemistry and Physics Discussions

The Sichuan Basin is among the most important areas of air pollution in China (Qiao et al., 2019;Gui et al., 2019;Zhong et al., 2019). Although there are many studies in this area, there are few long-term view studies of the hourly concentration data resolution of $PM_{2.5}$ chemical components. In this study, through long-term observations (from 1 January 2015 to 31 December 2017), we analysed the pollution level and chemical conversion characteristics of NSA in $PM_{2.5}$ in Chengdu and the concentration change sensitivities of sulfate, nitrate and ammonium. Finally, combined with local emissions and regional transmission characteristics, we analysed the regional transport characteristics of Chengdu air pollution.

## 2 Experiment and methods

### 2.1 Observation site

Comprehensive observations were carried out at the Super Station of Atmospheric Environmental Monitoring of Chengdu Academy of Environmental Protection Sciences (30.65°N, 104.05°E). The site is located in the Wuhou District of Chengdu, between First Ring Road and Second Ring Road (Fig. 1). This is a typical residential, transportation and commercial mixed area that represent the characteristics of the urban atmospheric environment. Chengdu is also a megacity in the Sichuan Basin of Southwest China, as well as an important part of the Chengdu-Chongqing region, which is among the regions with serious air pollution in China (Fig. 1).

https://doi.org/10.5194/acp-2019-1142
Preprint. Discussion started: 26 February 2020


Atmospheric Chemistry and Physics Discussions

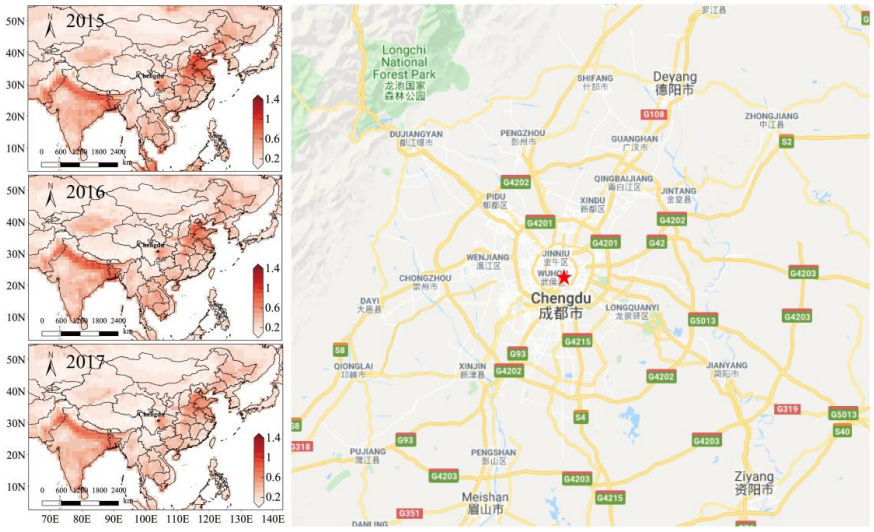


Fig. 1. Observation site in Chengdu. The image on the left shows the aerosol optical depth (AOD, 550 nm) from 2015 to 2017 (National Aeronautics and Space Administration, 2019, last access: 12 February 2020). The red star in the image on the right shows the location of the observation site in Chengdu (© Google Maps 2020).

**2.2 Instruments**

During the research period, online experimental monitoring instruments were used to obtain the observation data with an hourly resolution. The equipment list is shown in Table 1.

Table 1. The experimental instruments used in this study

| Instrument Model | Parameters | Manufacturer/Country |
|---|---|---|
| URG-9000 | $NO_3^-/SO_4^{2-}/NH_4^+/Na^+/Mg^{2+}/Ca^{2+}/Cl^-/K^+$ | Thermo Fisher Scientific/USA |
| SHARP 5030 | $PM_{2.5}/PM_1$ | Thermo Fisher Scientific/USA |
| RT-4 | OC/EC | Sunset Laboratory/USA |
| Xact-625 | Fe/Mn | CES/USA |
| 450i/17i/42iY/48i/49i | $SO_2/H_2S/NOx/NO_2/NO/NH_3$/ CO/$O_3$ | Thermo Fisher Scientific/USA |
| WXT520 | Meteorological parameters | VAISALA/Germany |

https://doi.org/10.5194/acp-2019-1142
Preprint. Discussion started: 26 February 2020


Atmospheric Chemistry and Physics Discussions

### 2.3 Chemical conversions and model methods

To examine the conversion of gaseous pollutants to secondary aerosols, the sulfur oxidation ratio (SOR) and nitrogen oxidation ratio (NOR) were used to reflect the conversions of $SO_2$ and $NO_2$ to sulfate and nitrate, respectively (Sun et al., 2014;Yang et al., 2015b). They can be calculated using Eq. (1) and Eq. (2):

$$SOR=nSO_4^{2-}/(nSO_4^{2-}+nSO_2) \quad (1)$$

$$NOR=nNO_3^-/(nNO_3^-+nNO_2) \quad (2)$$

where n is the molar concentration.

The ISORROPIA-II thermodynamic model was used to analyse the variation characteristics of the interaction among aerosol chemical components (Fountoukis and Nenes, 2007;Guo et al., 2017;Ding et al., 2019). Temperature (T), relative humidity (RH) and the total concentrations (i.e., gas + aerosol) of $Na^+$, $SO_4^{2-}$, $NH_3$, $NO_3^-$, $Cl^-$, $Ca^{2+}$, $K^+$ and $Mg^{2+}$ were input into the ISORROPIA-II thermodynamic model. In this study, we use "forward problems" mode to run the model, assuming that the aerosols were in a "metastable" state (salts do not precipitate under supersaturated conditions). The simulated data and observed data were compared and analysed. Simultaneously, the aerosol water content (AWC) and pH of aerosols were calculated. The sensitivity of the interaction between aerosol chemical components (NSA) was analysed (Ding et al., 2019;Fountoukis et al., 2009). The pH can be calculated using Eq. (3):

$$\mathrm{pH} = -log_{10}H_{aq}^{+} \cong -log_{10}\frac{1000H_{air}^{+}}{AWC} \quad (3)$$

where $H_{aq}^{+}$ (mol/L) is the concentration of hydronium ions in liquid water of atmospheric particulate matter, which can be calculated by the $H_{air}^{+}$ and AWC ($\mu g/m^3$) outputs from the ISORROPIA-II thermodynamic model (Ding et al., 2019;Guo et al., 2017).

Gas-particle phase partitioning can be used to describe the transformation characteristics between semivolatile inorganic salts ($NO_3^-$ and $NH_4^+$) and corresponding gases ($HNO_3$ and $NH_3$) (Guo et al., 2017), which can be calculated by Eq. (4) and Eq. (5):

https://doi.org/10.5194/acp-2019-1142
Preprint. Discussion started: 26 February 2020


Atmospheric Chemistry and Physics Discussions

$$\varepsilon(NO_3^-) = \frac{NO_3^-}{HNO_3+NO_3^-} \quad (4)$$

$$\varepsilon(NH_4^+) = \frac{NH_4^+}{NH_3+NH_4^+} \quad (5)$$

where the units of $NO_3^-$, $NH_4^+$, $NH_3$ and $HNO_3$ were μg/m$^3$, and the $HNO_3$ data are from the ISORROPIA-II thermodynamic model output.

**2.4 CPF and PSCF methods**

To analyse the relationship between pollutants and wind direction (WD) and wind speed (WS), the conditional probability function (CPF) was introduced the R Programming Language. This function can be defined as CPF= $m_{\theta,j}/n_{\theta,j}$, where $m_{\theta,j}$ is the number of samples in the WD interval θ and WS interval j with mixing ratios greater than some, given a 'high' pollution concentration (percentile of pollutants), and $n_{\theta,j}$ is the total number of samples in the same wind direction-speed interval (Uria-Tellaetxe and Carslaw, 2014). Usually, a higher given 'high' pollution concentration (percentile) is chosen, such as the 90th percentile, which will mask the lower percentile pollution concentration source contributions. In this work, to obtain a more complete contribution of pollution sources, a range of percentile values were selected for the CPF calculation, e.g. 0-25, 25-50, 50-75 and 75-100.

The potential source contribution function (PSCF) is based on the analysis of pollution sources, which is based on the airmass backward trajectory and can be used to judge the long-distance regional transport of pollutants (Ji et al., 2019). In this study, Meteoinfomap and TrajStat (Wang et al., 2009) were used, and the Hybrid Single-Particle Lagrangian Integrated Trajectory (HYSPLIT) data input model were provided by National Oceanic and Atmospheric Administration (National Oceanic and Atmospheric Administration, 2019, last access: 12 February 2020); these data was used for calculating the 24-hr backward trajectories at the observation site at a height of 500 m every 1 hr from 1 January 2015 to 31 December 2017 (UTC+8). The calculated domain for PSCF was a range of 20-50° N, 75-115° E, and a grid cell with a resolution of 0.5° ×0.5° was divided. The PSCF can be defined as Eq. (6):

https://doi.org/10.5194/acp-2019-1142
Preprint. Discussion started: 26 February 2020


Atmospheric Chemistry and Physics Discussions

$$PSCF_{ij} = \frac{M_{ij}}{N_{ij}} W_{ij} \quad (6)$$

$$W_{ij} = \begin{cases} 1.0 \left(N_{ij} \geq 3N_{ave}\right) \\ 0.7 \left(3N_{ave} > N_{ij} \geq 1.5N_{ave}\right) \\ 0.4 \left(1.5N_{ave} > N_{ij} \geq N_{ave}\right) \\ 0.2 \left(N_{ave} > N_{ij}\right) \end{cases} \quad (7)$$

where $PSCF_{ij}$ is the value for the ijth grid cell, $M_{ij}$ is the total number of endpoints in the ijth grid cell, with pollution concentrations at the observation site (30.65°N, 104.05°E) that are greater than a given threshold value (75 percentiles are selected for gaseous pollutants). $N_{ij}$ is the number of backward trajectory endpoints that fall in the ijth grid cell during the simulation period. To reduce the uncertainty in $N_{ij}$, an empirical weight function $W_{ij}$ was introduced in Eq. (7), where $N_{ave}$ is the average of $N_{ij}$ during the simulation period (Ji et al., 2019;Zhang et al., 2017;Wang et al., 2009).

## 3 Results and discussion

### 3.1 Pollution characteristics of the interannual and entire observation periods

The annual average mass concentration of NSA and its proportion in $PM_{2.5}$ are shown in Table 2. The annual averages of $PM_{2.5}$ were 67.78, 71.88 and 59.68 μg/m$^3$, corresponding to 2015, 2016 and 2017, respectively. However, the pollution of $PM_{2.5}$ in Chengdu was much higher than the annual secondary guideline value (35 μg/m$^3$, Ambient air quality standards/GB3095-2012) and the World Health Organization annual guideline value (10 μg/m$^3$). The same $PM_{2.5}$ pollution problem was also a serious problem in Beijing and Nanjing (Ji et al., 2019;Zheng et al., 2019). The annual average mass concentration of NSA also changed significantly, and the difference was large. The Mann-Whitney U test showed that the variation in $NO_3^-$ was nonsignificant ($p > 0.05$), and $SO_4^{2-}$ and $NH_4^+$ had obvious significance from 2015 to 2017 ($p < 0.05$), indicating that $NO_3^-$ had not decreased significantly, and there was an increase in 2017 compared to 2015. $SO_4^{2-}$ continues to decline, and $NH_4^+$ was also lower in 2017 compared to 2016. Notably, $SO_4^{2-}$ and $NH_4^+$ decreased significantly in 2017 compared with 2015, but the variation in $NO_3^-$ was nonsignificant. Meanwhile, the annual averages of $NO_3^-/SO_4^{2-}$ were 0.95, 1.02 and 1.45 for 2015, 2016 and 2017, respectively,

https://doi.org/10.5194/acp-2019-1142
Preprint. Discussion started: 26 February 2020


Atmospheric Chemistry and Physics Discussions

indicating that the contribution of vehicle emissions as a mobile source to $PM_{2.5}$ was increased compared with that of coal combustion as a stagnant source (Li et al., 2017;Wang et al., 2015). As shown in Table S1, from 2013 to 2017, the emissions of $NO_2$ in Chengdu were obviously higher than those of $SO_2$, but $PM_{2.5}$, $NO_2$ and $SO_2$ all showed downward trends, which benefited from the implementation of the Air Pollution Prevention and Control Action Plan launched by the Chinese government, and Chengdu also launched a more detailed pollution control plan in 2014 (the People's government of Chengdu, 2014, last access: 12 February 2020).

Table 2. Comparison of annual mass averages ($\mu g/m^3$) and proportions (%) for NSA from 2015 to 2017.

| | $NO_3^-$ | $SO_4^{2-}$ | $NH_4^+$ | $PM_{2.5}$ | $NO_3^-/PM_{2.5}$ | $SO_4^{2-}/PM_{2.5}$ | $NH_4^+/PM_{2.5}$ |
|---|---|---|---|---|---|---|---|
| 2015 | 9.13 | 10.37 | 6.14 | 67.78 | 0.129 | 0.165 | 0.088 |
| 2016 | 9.27 | 8.53 | 6.16 | 71.88 | 0.123 | 0.133 | 0.089 |
| 2017 | 9.17 | 6.88 | 5.01 | 59.68 | 0.141 | 0.132 | 0.079 |

https://doi.org/10.5194/acp-2019-1142
Preprint. Discussion started: 26 February 2020


Atmospheric Chemistry and Physics Discussions

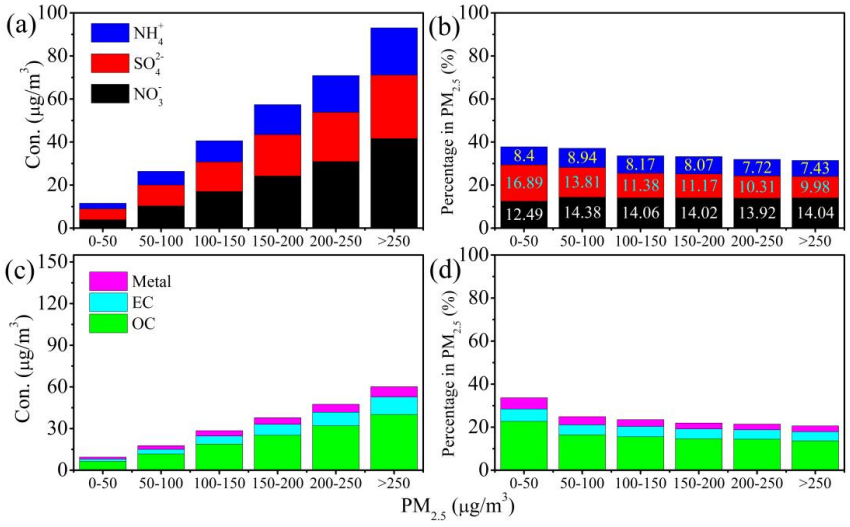


Fig. 2. Variation characteristics of the NSA and other chemical compositions with different concentrations of $PM_{2.5}$. (a) NSA mass concentration. (b) Percentage of NSA in $PM_{2.5}$. (c) Chemical compositions of organic carbon (OC), element carbon (EC), and metal elements. (d) Percentage of other chemical compositions in $PM_{2.5}$.

The chemical composition of $PM_{2.5}$ from 2015 to 2017 varies with its concentration, as shown in Fig. 2. With the accumulation of $PM_{2.5}$ in the atmosphere, the concentration of NSA has also increased significantly, but their proportion in $PM_{2.5}$ has a downward trend (Fig. 2a and b). When the $PM_{2.5}$ was less than 50 μg/m$^3$ and greater than 250 μg/m$^3$, the mass concentrations of NSA were 11.57 and 90.06 μg/m$^3$, respectively, and the proportions were 37.78 and 31.45% respectively. Comparing Fig. 2b and d, it was found that NSA was always the main contributor in the entire process of $PM_{2.5}$ accumulation, which was significantly higher than the proportions of OC and EC (Ji et al., 2019;Li et al., 2019c). In the accumulation process of $PM_{2.5}$ concentrations greater than 50 μg/m$^3$, nitrate accounts for a high proportion in NSA and was stable at approximately 14%, and the proportion of sulfate and ammonium continues to decrease (Li et al., 2019c;Wang et al., 2016). When the $PM_{2.5}$ concentration was less than 50 μg/m$^3$, the concentration of $SO_4^{2-}$ was higher than that of $NO_3^-$, and the concentration

https://doi.org/10.5194/acp-2019-1142
Preprint. Discussion started: 26 February 2020


Atmospheric Chemistry and Physics Discussions

of $NH_4^+$ was lower than the $NH_4^+$ concentration of $PM_{2.5}$ at 50 to 100 μg/m$^3$, possibly due to sulfate concentration was higher than nitrate, forming more chemically stable ammonium sulfate (Guo et al., 2017). In addition, when $PM_{2.5}$ was less than 50 μg/m$^3$, low RH and strong solar radiation were also important ways to generate sulfate (Yao et al., 2018).

### 3.2 Monthly and seasonal variations

The monthly variation characteristics of NSA from 2015 to 2017 are shown in Fig. 3. These variations have similar trends due to meteorological factors (Fig. S1); from April to August, they have higher temperature and WS, lower RH and atmospheric pressure, which is not only conducive to the dilution and diffusion of pollutants but also reduces the chemical conversions of pollutants by aqueous phase and the concentrate ability of gaseous pollutants to concentrate particles (Wang et al., 2016;Ji et al., 2019). Overall, the concentrations are higher in January and December and lower in July and August. The highest monthly average of $NO_3^-$ reached 19.98 μg/m$^3$ in January 2017, and the highest monthly average of $SO_4^{2-}$ and $NH_4^+$ were 22.08 μg/m$^3$ and 12.66 μg/m$^3$ in January 2015, respectively. The lowest concentrations of NSA appeared in August 2017, which were 1.96, 3.07 and 1.62 μg/m$^3$. The gaseous precursors of NSA also have obvious monthly variations, and the NOx and $SO_2$ trends were similar to those of nitrate and sulfate (Fig. 3 and S2). $NH_3$ emissions were significantly different, with increases in warmer months (April-July) and colder months (September-December). On the one hand, $NH_3$ volatilization was promoted by relatively high temperatures; on the other hand, the use of agricultural fertilizers and livestock farming were also important sources of $NH_3$ in China. Second, from urban areas, fossil fuel combustion and motor vehicle emissions also contribute significantly (Liu et al., 2013a;Pan et al., 2016). Notably, $NH_3$ increased significantly from April to December 2017 compared with 2015 and 2016, especially during low-temperature months (Fig. S2c). This also shows that the implementation of air pollution reduction measures should increase the emission reduction intensity in terms of NOx and $NH_3$ emissions, especially the

https://doi.org/10.5194/acp-2019-1142
Preprint. Discussion started: 26 February 2020


Atmospheric Chemistry and Physics Discussions

implementation of autumn and winter air pollution prevention and control action. The seasonal variation in NSA was shown in Fig. S3, and the concentration in winter was much higher than that in summer. Nitrate only declined in spring and summer from 2015 to 2017, with an increase in autumn and winter (Fig. S3a). Seasonal variations in ammonium were similar to those of nitrates, with higher concentrations in winter and the lowest in summer. This may be because higher temperatures and WSs not only can promote the decomposition of ammonium nitrate in summer but also promote the dilution and diffusion of pollutant concentrations (Guo et al., 2017;An et al., 2019). Sulfate has a significant downward trend in all seasons from 2015 to 2017, especially in winter. This downward trend was due to implementation of the Air Pollution Prevention and Control Action Plan, especially the measures of "electricity instead of coal" and "natural gas instead of coal" (refers to increased use of electricity and natural gas in the residential sector to reduce coal combustion). The variation amplitude of NSA and gaseous pollutants in cold months was significantly higher than that in warm months (Figs. 3, S2 and S3). This higher variation amplitude may be due to the differences in pollutant accumulation and scavenging processes. This finding also indicates that the instability of local pollutant emissions and regional transport during cold months was affected by meteorological conditions (Li et al., 2017;Ji et al., 2018). The large variation amplitude of pollutants in different months, similar to the changes in the Beijing-Tianjin-Hebei region of northern China and Chengdu, are due to the accumulation and removal of pollution by meteorological conditions and pollutants emissions (Ji et al., 2019;Qin et al., 2019;Zhang et al., 2019).

https://doi.org/10.5194/acp-2019-1142
Preprint. Discussion started: 26 February 2020


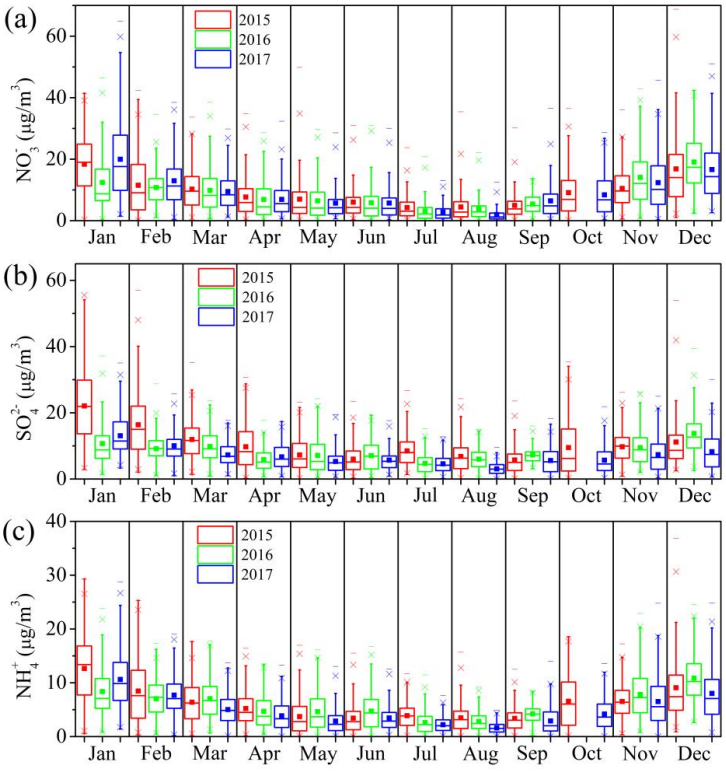


**Fig. 3. Monthly variations in $NO_3^-$, $SO_4^{2-}$ and $NH_4^+$ mass concentrations from 2015 to 2017.3.3 Diurnal and weekly variations**

The diurnal variation in NSA is shown in Fig. 4; a similar trend was shown for daily changes of nitrate, sulfate and ammonium, which was higher in the daytime than in the evening. From 2015 to 2017, the diurnal variation trend of nitrate was similar, sulfate was obviously reduced, and the ammonium was only significantly reduced in 2017. The decrease in $NH_4^+$ may be closely related to the decrease in $SO_4^{2-}$ (Fig. 4a). Some studies have shown that $NH_4^+$ in aerosols will first combine with $SO_4^{2-}$ ions and $HSO_4^-$ to form $(NH_4)_2SO_4$ or $NH_4HSO_4$ and then combine with $NO_3^-$. The significant drop in $NH_4^+$ in 2017 may be due to a decrease in $SO_4^{2-}$. Similarly, the $NH_4^+$ did not show a significant decrease in 2016, probably due to the increase in $NO_3^-$ in 2016 (Table 2), combined with a portion of the $NH_4^+$ (Meier et al., 2009;Sun et al., 2014;Ding et al., 2019). This

https://doi.org/10.5194/acp-2019-1142
Preprint. Discussion started: 26 February 2020


Atmospheric Chemistry and Physics Discussions

finding also indicates that the concentration of $NH_4^+$ in particulate matter in Chengdu may be affected by the concentration of $SO_4^{2-}$. From 2015 to 2017, the concentration of NSA was higher in the daytime than in the evening (Fig. 4a), and similar results were found in different seasons (Fig. 4b), which may be due to the combination of pollutant emissions and meteorological conditions. As shown in Fig. S4, from 9:00 to 11:00 a.m., the concentrations of $SO_2$, NOx, $NH_3$, CO and other gases increased significantly, indicating that the primary emission of pollutants was relatively strong. At this time, higher RH (Fig S5) also provides favourable conditions for the formation of secondary aerosols and promotes the accumulation of NSA (Cheng et al., 2016;Wang et al., 2016;Sun et al., 2014). In addition, before 10 o'clock, relatively low WS will enable easy pollutant concentration accumulation. In contrast, the higher WS in the afternoon may be the main factor for the decrease in pollutant concentration (Fig. 4, S4 and S5). Photochemical reactions may also be one of the factors in the formation of NSA, and the concentration of $O_3$ peaks at approximately 15:00, which may be affected by the free radicals generated by photochemistry. At approximately 19:00, the ratio of $NO_2$/NO reached its highest value, and the concentration of $NO_2$ also increased significantly (Song et al., 2018;Zhu et al., 2019). At night, with the increase in RH (Fig. S5), dissolved ozone, free radicals, hydrogen peroxide and $NO_2$ can catalyse $SO_2$ to form secondary aerosols through an aqueous phase reaction (Zhang et al., 2015;An et al., 2019). The seasonal diurnal variation in NSA was shown in Fig. 4b. The concentration of NSA in winter was obviously higher than that in summer, and the diurnal variation range was larger. The concentration in spring and autumn was closer, but the diurnal variation in spring was larger than that in autumn. The larger diurnal variation range not only indicates serious pollution but also indicates the importance of other factors affecting air quality, such as meteorological conditions, secondary aerosol conversion conditions, and so on (Ji et al., 2019;Yang et al., 2015a). The peak value of the NSA seasonal diurnal variation also varies in different seasons. The peak value appears at approximately 13:00 in winter, approximately 10:00 in spring and summer,

https://doi.org/10.5194/acp-2019-1142
Preprint. Discussion started: 26 February 2020


Atmospheric Chemistry and Physics Discussions

and approximately 12:00 in autumn, possibly due to the influence of meteorological conditions.

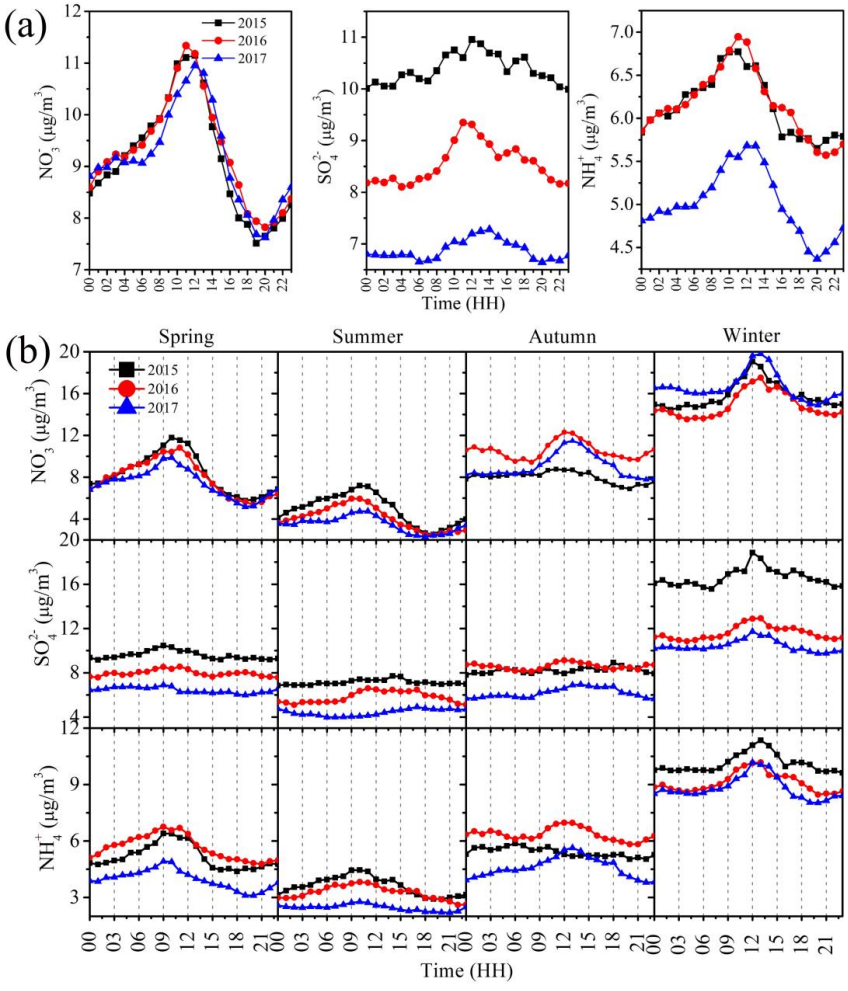


Fig. 4. Diurnal variations in NSA from 2015 to 2017. (a) Annual average. (b) Seasonal average.

The weekly variation in NSA is shown in Figs. S6-8. During the overall observational period, workdays (Monday to Friday) showed higher variations than the weekend (Saturday and Sunday), with the highest variation being on Tuesday and the lowest being on Sunday. Despite the difference in mean values between Tuesday and Sunday, nonparametric tests show that the difference in mean values was nonsignificant (Mann-

https://doi.org/10.5194/acp-2019-1142
Preprint. Discussion started: 26 February 2020


Atmospheric Chemistry and Physics Discussions

Whitney U test, $P > 0.05$). As shown in Figs. S6-7, the average trends of $NO_3^-$ and $NH_4^+$ were consistent from Monday to Sunday. The correlation coefficient was 0.94 ($P < 0.01$) from 2015 to 2017, which indicates that they have a common source and that the vehicle emissions also have an important contribution to $NH_4^+$ (Pan et al., 2016). The average values of $NO_3^-$, $SO_4^{2-}$ and $NH_4^+$ from 2015 to 2017 were 9.21, 8.64 and 5.64 ug/m$^3$ on workdays and 8.56, 8.33 and 5.29 ug/m$^3$ on weekends, respectively. Similarly, the Mann-Whitney U test showed no significant difference. Population standard deviation comparisons of $NO_3^-$, $SO_4^{2-}$ and $NH_4^+$ showed that workdays were higher than weekends, with 7.96, 6.04 and 4.35 on weekdays, 6.76, 5.69 and 3.88 on weekends, respectively (Fig. S8). Compared with the diurnal variations on weekdays and weekends, the variations in nitrate and ammonium were more obvious than those of sulfate (Fig. S9). In Beijing, a vehicle restriction scheme based on motor vehicle license plates was implemented, that is, there are no restrictions on weekends, and the contribution of vehicle emissions pollution on weekends was lower than that on workdays (Ji et al., 2019). Similarly, Chengdu also implemented restriction measures according to the license plate of vehicles on weekdays, but the average concentration of pollutants on weekdays was slightly higher than that on weekends (Mann-Whitney U test, $P > 0.05$). This finding shows that while implementing a policy of motor vehicle restriction, improving the emission standards of motor vehicles and the quality of gasoline and diesel oil was an important measure.

### 3.4 Chemical characteristics of NSA

#### 3.4.1 Relationship between NSA and carbonaceous components

Precursor gases of NSA, such as $SO_2$, NOx and $NH_3$, are usually derived from coal combustion, vehicle exhaust and agricultural sources, and they are accompanied by emissions of carbonaceous aerosols (Wang et al., 2016). Fig. 5a, b and c show the relationship between NSA concentration and CO, OC and EC, demonstrating a good Pearson's correlation ($p<0.01$), which indicates that the emissions of carbon aerosols were accompanied by the emissions of NSA precursor gases; these gases form NSA

https://doi.org/10.5194/acp-2019-1142
Preprint. Discussion started: 26 February 2020


Atmospheric Chemistry and Physics Discussions

through complex chemical reactions, such as photochemical, aqueous chemical conversions and heterogeneous reactions (An et al., 2019;Li et al., 2019a;Zhu et al., 2019). CO and EC usually originate from combustion sources, while OC originates from primary emissions and secondary conversion (Tie et al., 2017;Tao et al., 2017;Kong et al., 2019;Wu et al., 2016). The OC/EC value can be used to determine the sources of carbon aerosols, such as vehicle exhaust, coal combustion and biomass burning (Zhang et al., 2010). As shown in Fig. 5d, when the concentration of nitrate and ammonium reached a peak, the OC/EC value was between 2-3, which was lower than the OC/EC value when the sulfate was at the peak (3-4). Previous studies have also shown that the OC/EC value of vehicle emissions was lower than that of coal combustion (Cao et al., 2005;Kopp and Mauzerall, 2010). Nitrate and ammonium also have similar trends, and their Pearson's correlation was 0.92 ($p<0.01$), which was higher than that of ammonium and sulfate (0.88). The correlation coefficients of $NH_3$ with NOx and $SO_2$ were 0.42 and 0.23, respectively, suggesting that vehicle emissions may also be a major source of ammonia (Pan et al., 2016;Liu et al., 2013a).

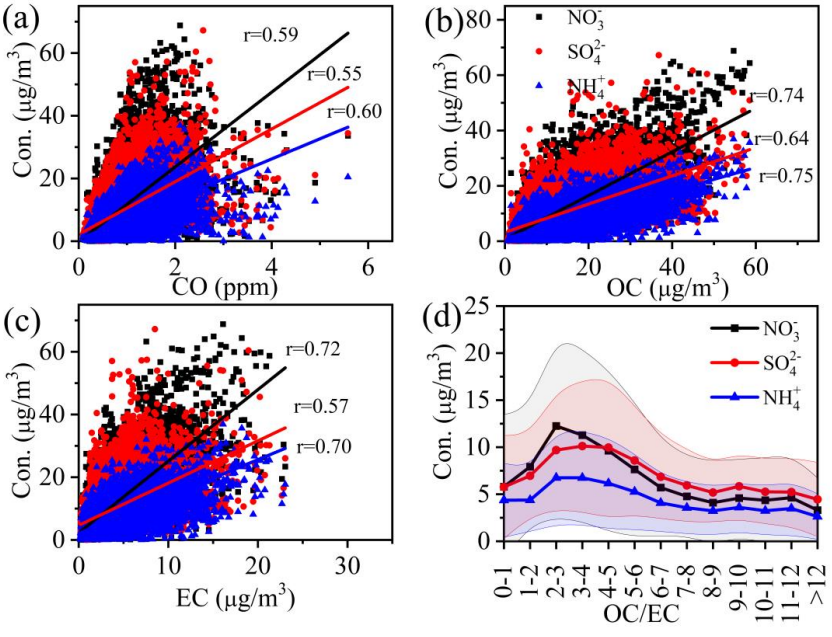

https://doi.org/10.5194/acp-2019-1142
Preprint. Discussion started: 26 February 2020




Fig. 5. Relationships between NSA and CO and OC and EC. (a) NSA and CO. (b) NSA and OC. (c) NSA and EC. (d) NSA and OC/EC.

**3.4.2 Chemical conversion characteristics of NSA**

Figure 6 shows the abilities of $SO_2$ and $NO_2$ to chemically convert to sulfates and nitrates and the variation trend of ozone concentration and metal elements at different $PM_{2.5}$ concentrations. With the increase in $PM_{2.5}$ concentration, SOR and NOR gradually increased, indicating that the formation ability of sulfate and nitrate increased during the formation of air pollution. As the concentration of $PM_{2.5}$ increases, the extinction properties of aerosols increase, the photochemical reaction conditions weaken, and the $O_3$ concentration shows a decreasing trend, as shown in Fig. 6a. With the accumulation of $PM_{2.5}$ concentration, metal elements (Fe and Mn) also showed an increasing trend and were similar to SOR and NOR. Previous studies have shown that mineral dust elements such as Fe and Mn can play a catalytic role in the formation of atmospheric sulfate (Martin and Good, 1991;He et al., 2014). The Pearson's correlation statistics of SOR and NOR with Fe and Mn under different $PM_{2.5}$ concentration conditions are shown in Table S2; it is only under high $PM_{2.5}$ concentration conditions (>200 $\mu g/m^3$) that SOR and NOR have a positive correlation. This result is similar to those of previous studies in Beijing and Xi'an, where Fe and Mn play a limited catalytic role in sulfate formation (Cheng et al., 2016;Wang et al., 2016). Some studies suggest that when SOR is greater than 0.1, there may be a photochemical reaction pathway leading to the conversion of $SO_2$ to sulfate (Ohta and Okita, 1990). Fig. 6a shows that in addition to the photochemistry contributing to $SO_2$ oxidation, there may be a more important pathway leading to the conversion of $SO_2$ to sulfate.

https://doi.org/10.5194/acp-2019-1142
Preprint. Discussion started: 26 February 2020


Atmospheric Chemistry and Physics Discussions

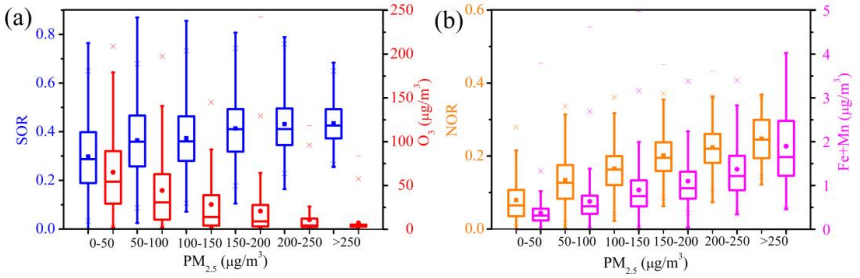


Fig. 6. Analysis of atmospheric chemical conversion ability at different $PM_{2.5}$ concentrations. (a) SOR and $O_3$. (b) NOR and concentration of metal elements (Fe and Mn).

Figure 7 shows the variation characteristics of NSA chemical conversions and meteorological conditions with increasing RH. SOR and NOR increased with increasing RH, suggesting that $SO_2$ and $NO_2$ were more likely to produce sulfate and nitrate under higher RH conditions. Previous studies have shown that in the presence of $NH_3$, $NO_2$ can promote the chemical conversion of $SO_2$ to sulfate in the aqueous phase (Wang et al., 2016). In aerosol water, alkaline aerosol components can promote the dissolution of $SO_2$ and formation of sulfate under the oxidation of $NO_2$ (Cheng et al., 2016). Especially when the atmosphere was polluted, the formation of sulfate by $SO_2$ through the aqueous phase environment can contribute most of the sulfate (Sun et al., 2013). According to the ISORROPIA-II thermodynamic model simulation, AWC and pH also increase with RH (Fig. 7c and d). The increase in AWC can dilute the concentrations of sulfate and hydrogen ions and promote an equilibrium shift in the $SO_2$ to sulfate during the aqueous phase. The increase in RH and gradual decrease in T can also affect the gas-particle phase partitioning of $HNO_3$-$NO_3^-$ (Fig. 7g) and $NH_3$-$NH_4^+$ (Fig. 7h), prompting more nitrate and ammonium to condense in aerosol liquid water. By comparing the NOR with the meteorological conditions and gas-particle distribution when RH is greater than 80% (Fig. 7b, e, f and g), the increase in T and the decrease in atmospheric pressure were not conducive to the conversion and presence of nitrate in the aqueous phase (Guo et al., 2017;Ding et al., 2019). Therefore, Figs. 6 and 7 also

https://doi.org/10.5194/acp-2019-1142
Preprint. Discussion started: 26 February 2020


Atmospheric Chemistry and Physics Discussions

illustrate that the aqueous phase oxidation environment may contribute to the generation of a larger portion of NSA.

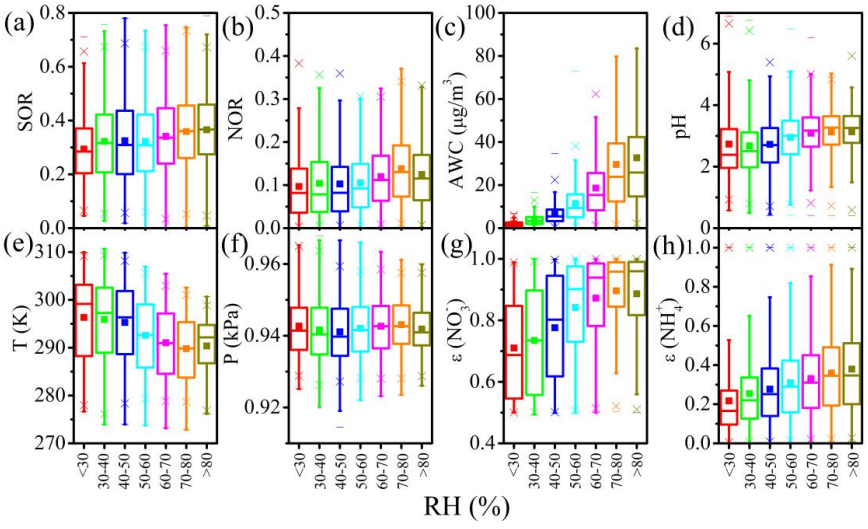


Fig. 7. Effects of RH on the chemical conversion of NSA. (a) SOR. (b) NOR. (c) AWC. (d) pH of $PM_{2.5}$. (e) Temperature (T). (f) Atmospheric pressure (P). (g) $NO_3^-$ gas-particle phase partitioning. (h) $SO_4^{2-}$ gas-particle phase partitioning.

**3.4.3 Sensitivity analysis**

The molar ratio analysis of NSA shown in Fig. 8 was used to analyse the chemical relationships among NSA. $(NH_4)_2SO_4$ and $NH_4NO_3$ are mainly composed of $NH_4^+$, $SO_4^{2-}$ and $NO_3^-$ in particulate matter (Malm and Hand, 2007;Meier et al., 2009). Because $(NH_4)_2SO_4$ has better stability than $NH_4NO_3$, $NH_4^+$ will first combine with $SO_4^{2-}$ and then with $NO_3^-$ (Liu et al., 2012). The annual average molar ratio of $NH_4^+$ to $2*SO_4^{2-}$ was more than 1, which indicates that $SO_4^{2-}$ can be completely neutralized by $NH_4^+$ (Fig. 8a). The molar ratios of residual $NH_4^+$ ($NH_4^+$ - $2*SO_4^{2-}$) to $NO_3^-$ were 0.93, 0.99 and 1.05 in 2015, 2016 and 2017, respectively. As shown in Fig. 8a and b, the gradual increase in the ratio (slope k) from 2015 to 2017 indicates an increase in ammonia emissions from aerosols, especially in 2017, with a ratio of 1.05, indicating the presence of other forms of ammonium salts, such as $NH_4Cl$ and $(NH_4)_2C_2O_4$ (Sun

https://doi.org/10.5194/acp-2019-1142
Preprint. Discussion started: 26 February 2020


Atmospheric Chemistry and Physics Discussions

et al., 2006). Seasonal variations in $NH_4^+$, $SO_4^{2-}$ and $NO_3^-$ are shown in Fig. 8c and d. The higher molar ratio in autumn indicates that the intensity of ammonia emission in autumn was higher than that in other seasons. This finding also shows that the problem of atmospheric ammonia-rich environments in Chengdu in 2017 and autumn was more prominent.

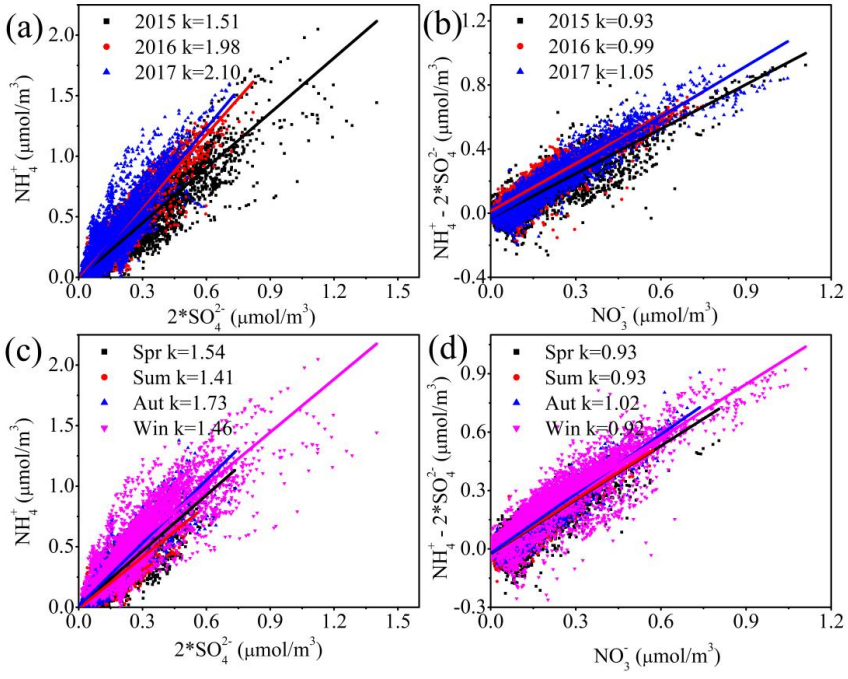


Fig. 8. Molar ratio analysis of NSA. (a) Interannual variation in the molar ratio of $SO_4^{2-}$ and $NH_4^+$. (b) Interannual variation in the molar ratio of $NO_3^-$ and $NH_4^+$. (c) Seasonal variation in the molar ratio of $SO_4^{2-}$ and $NH_4^+$. (d) Seasonal variation in the molar ratio of $NO_3^-$ and $NH_4^+$.

Table 3 shows the sensitivity analysis of the concentration variations in $SO_4^{2-}$, $NO_3^-$ and $NH_4^+$. ISORROPIA-II thermodynamic model sensitivity analysis is described in detail in the Supplementary Materials. The coefficient of variance represents the response of the species to variations in other components. The coefficients of variance for $NH_4^+$ and $NO_3^-$ produced by $SO_4^{2-}$ changes were 52.62 and 5.38, respectively. Similarly, the

https://doi.org/10.5194/acp-2019-1142
Preprint. Discussion started: 26 February 2020


Atmospheric Chemistry and Physics Discussions

480 coefficients of variance for $NH_4^+$ and $SO_4^{2-}$ produced by nitrate changes are 49.27 and
481 0.002, respectively. The large coefficient of variance for $NH_4^+$ indicates that the changes
482 in $SO_4^{2-}$ and $NO_3^-$ can affect the presence of $NH_4^+$, which also indicates that $(NH_4)_2SO_4$
483 and $NH_4NO_3$ were the main states of $NH_4^+$ (Liu et al., 2012). The coefficients of
484 variance for $SO_4^{2-}$ and $NO_3^-$ produced by $NH_3$ changes are 2.48 and 31.30, respectively,
485 which indicates that $NH_4^+$ was excessive to sulfate and that $NH_4^+$ first combines with
486 sulfate to form stable $(NH_4)_2SO_4$, and the remaining $NH_4^+$ and $NO_3^-$ will combine to
487 form $NH_4NO_3$. From 2015 to 2017, the coefficient of variance for $NH_4^+$ and $NO_3^-$
488 caused by the changes in $SO_4^{2-}$ gradually decreased, which may be attributed to the
489 decrease in $SO_4^{2-}$ concentration in $PM_{2.5}$ (Table 2). The coefficients of variance for $NO_3^-$
490 caused by the changes in $NH_3$ in 2015 and 2016 were 32.83 and 38.24, respectively. At
491 this time, $NO_3^-$ can completely neutralize $NH_4^+$. In 2017, the coefficient of variance
492 was 21.88, and the ammonia was a surplus (Fig. 8b); thus, the coefficient of variance
493 may be affected by the thermal instability of $NH_4NO_3$ during this time (Ansari and
494 Pandis, 2000;An et al., 2019). In terms of seasonal variation, the changes in sulfate and
495 nitrate can cause larger coefficients of variance for $NH_4^+$. When $NH_3$ changes, the
496 coefficient of variance for $NO_3^-$ was greater than that of $SO_4^{2-}$. In summer, the
497 coefficient of variance for $NO_3^-$ and $NH_4^+$ caused by the changes in $SO_4^{2-}$ were
498 obviously higher than those in other seasons. On the one hand, this may be due to the
499 relatively low concentrations of $NO_3^-$ and $NH_4^+$ in $PM_{2.5}$ due to lower gas-particle phase
500 partitioning in summer (Fig. S10a and b). On the other hand, the stronger
501 photochemical reaction may also lead to a greater change in the concentrations of $NO_3^-$
502 and $NH_4^+$ (Ohta and Okita, 1990). The coefficients of variance for $NO_3^-$ and $SO_4^{2-}$ in
503 winter were 6.13 and 0.005, respectively, which are higher than those in spring and
504 autumn, most likely due to higher NOR and SOR (Fig. S10c and d). Previous studies
505 have shown that the conversion of $SO_2$ to sulfate in the aqueous phase not only increases
506 the conversion of sulfate but also enhances the formation of nitrate particles in the
507 aqueous phase (Wang et al., 2016). Therefore, sulfate emission reduction may play a

https://doi.org/10.5194/acp-2019-1142
Preprint. Discussion started: 26 February 2020


Atmospheric Chemistry and Physics Discussions

key role in the process of controlling emission reduction in NSA pollution, as it not only reduces the presence of $NH_4^+$ ($(NH_4)_2SO_4$) in particulate matter but also affects the formation of $NH_4NO_3$ by influencing the formation of nitrate. $NO_2$ and $NH_3$ can also promote the conversion of $SO_2$ to sulfate through an aqueous phase environment (Wang et al., 2016). Therefore, in the current ammonia-rich environment, priority control of $SO_2$ and $NO_2$ emissions is an important way to reduce NSA in particulate matter. Through the implementation of the Air Pollution Prevention and Control Action Plan, the reduction in sulfate emissions has achieved good results. Therefore, while continuing to promote "electricity instead of coal" and "natural gas instead of coal" to reduce coal combustion pollution, more stringent control measures should be added for nitrate and ammonia emissions. To further improve air quality, the Chinese government launched a “Three-Year Action Plan for Winning the Blue Sky Defense Battle” in 2018 (the Sate Council, 2018) and proposed emission reduction targets for $SO_2$ and NOx emissions, which will be 15% lower in 2020 than in 2015. By using the ISORROPIA-II thermodynamic model to simulate $SO_4^{2-}$, $NO_3^-$ and $NH_3$ emission reduction control effects of 5%, 10%, 15% and 20% respectively, the results were shown in Table S3. The results show that a better effect can be achieved by controlling the $SO_4^{2-}$ and $NO_3^-$ emissions reduction, especially the effects of synergistic emissions reduction.

In addition, NSA can increase the hygroscopicity properties of aerosols, and more AWC can increase the pH by diluting the hydrogen ion concentration (Kong et al., 2020;Ding et al., 2019). Higher sulfates, nitrates and AWC correspond to a lower pH, indicating that higher sulfates and nitrates have a greater effect on increasing aerosol acidity than AWC dilution (Fig. S11a and b). Previous studies have also shown that sulfate formation reduces aerosol pH (Sun et al., 2014). The same increase in ammonia emissions can increase the aerosol pH (Fig. S11c). Table S3 also shows the impacts of $SO_2^-$, $NO_3^-$ and $NH_3$ emissions reduction control on pH, such as sulfate and nitrate emissions reduction increasing pH and $NH_3$ emissions reduction reducing pH, and synergistic emission reduction has the least impact on pH changes, so controlling the

https://doi.org/10.5194/acp-2019-1142
Preprint. Discussion started: 26 February 2020


Atmospheric Chemistry and Physics Discussions

536 emissions reduction ratio in the air pollutant emission reduction scheme to reduce the
537 impacts of aerosol pH is worth further study. Acid rain is mostly concentrated in
538 southern China, and there are also important acid rain problems in the Sichuan Basin
539 (Fig. S12). Therefore, while controlling NSA emissions, especially controlling
540 ammonia emissions, the potential environmental problems of acid rain are worth
541 comprehensive assessment and analysis (Liu et al., 2019c).

542 Table 3. Sensitivity analysis of NSA concentration variations during the different
543 observation periods.

| Periods | Variables | Coefficient of variance | | |
|---|---|---|---|---|
| | | $NO_3^-$ | $SO_4^{2-}$ | $NH_4^+$ |
| 2015-2017 | $NO_3^-$ | | 0.002 | 49.27 |
| | $SO_4^{2-}$ | 5.38 | | 52.62 |
| | $NH_3$ | 31.3 | 2.48 | |
| 2015 | $NO_3^-$ | | 0.005 | 43.34 |
| | $SO_4^{2-}$ | 11.27 | | 58.37 |
| | $NH_3$ | 32.83 | 2.69 | |
| 2016 | $NO_3^-$ | | 0.004 | 46.27 |
| | $SO_4^{2-}$ | 5.55 | | 45.15 |
| | $NH_3$ | 38.24 | 3.09 | |
| 2017 | $NO_3^-$ | | 0.001 | 58.22 |
| | $SO_4^{2-}$ | 2.56 | | 43.64 |
| | $NH_3$ | 21.88 | 1.23 | |
| Spring | $NO_3^-$ | | 0.001 | 40.55 |
| | $SO_4^{2-}$ | 3.5 | | 49.72 |
| | $NH_3$ | 26.57 | 2.49 | |
| Summer | $NO_3^-$ | | 0.002 | 34.69 |
| | $SO_4^{2-}$ | 27.85 | | 86.23 |
| | $NH_3$ | 58.29 | 1.74 | |
| Autumn | $NO_3^-$ | | 0.002 | 47.34 |
| | $SO_4^{2-}$ | 2.71 | | 49.18 |
| | $NH_3$ | 32.3 | 1.87 | |
| Winter | $NO_3^-$ | | 0.005 | 35.94 |
| | $SO_4^{2-}$ | 6.13 | | 36.08 |
| | $NH_3$ | 26.76 | 1.56 | |

Coefficient of variance: Standard deviation/Mean value*100

https://doi.org/10.5194/acp-2019-1142
Preprint. Discussion started: 26 February 2020


Atmospheric Chemistry and Physics Discussions

### 3.5 Characteristics of local emissions and regional transport

#### 3.5.1 Local emissions

The concentration of pollutants is obviously affected by meteorological conditions; for example, WS and WD can affect the accumulation and removal of pollutants (Li et al., 2016). Figs. S13-15 show the annual variation characteristics of NSA and gas precursors affected by the WS and WD using CPF. Overall, the higher WS was accompanied by a lower pollutant concentration. As the WS decreases, the pollution becomes serious, and the pollution hot spots were gradually concentrated. On the whole, when the WS was usually greater than 2 m/s, the pollution was light (pollutant concentration percentile was between 0-25). When WS was usually less than 1 m/s, the pollution was heavy (pollutant concentration percentile was between 75-100), the which also reflects the distance and orientation between the emission source and the observation station, indicating that when the pollution was serious, the contribution of local source emissions was more prominent.

Nitrate and NOx have similar distributions of pollution hot spots in the polar plot diagram (Fig. S13), and when the concentration percentile was between 0-25, they were concentrated in the northeast and southeast directions and widely distributed. When the concentration percentile was between 25-75, the sources of nitrate and NOx were distributed west and northeast of the observatory, and there were important contribution sources in the northwest direction (WS was approximately 3-4 m/s) in 2017. When the WS was approximately 1-2 m/s and the concentration percentile was between 50-75, the important NOx source was in the northwest direction. When the accumulation of pollution concentration was high (concentration percentile was between 75-100), the nitrate source was mainly concentrated in the east and southeast of the observation station, and NOx was distributed in the south and southeast, with WSs of less than 1 m/s; additionally, the distribution of pollution hot spots was relatively wide in 2016 (the annual mean values of NOx were 42.15, 43.99 and 39.63 (ppb) in 2015, 2016 and 2017, respectively). The sulfate and $SO_2$ pollution sources affected by meteorological

https://doi.org/10.5194/acp-2019-1142
Preprint. Discussion started: 26 February 2020


Atmospheric Chemistry and Physics Discussions

conditions also have similar distribution characteristics (Fig. S14). At a higher concentration of pollutants, the pollution hot spots of sulfate were distributed in the east and southeast of the observation station, and $SO_2$ was distributed in the northeast, southeast and west. The concentrations of $SO_2$ were 5.44, 4.15 and 3.68 (ppb) in 2015, 2016 and 2017, respectively. Compared with 2017 and 2016, the distribution of $SO_2$ pollution sources in 2016 was also more extensive, mainly in the west and northeast. The $NH_3$ emissions were slightly different from those of $SO_2$ and NOx (Fig. S15). Under conditions of high pollution concentration (concentration percentile was between 75-100), the pollution hot spots were distributed in the west in 2015 (WS was approximately 2-3 m/s), in the north in 2016 (WS was approximately 3 m/s), and in the near distance in 2017 (WS was approximately 0.5 m/s). The higher pollution concentration was accompanied by a higher WS (2015 and 2016), which indicates that the $NH_3$ emission transport in the surrounding area was more obvious, which may come from the surrounding agricultural source distribution area (Liu et al., 2019b;Liu et al., 2013a). The annual mean value of $NH_3$ emissions in 2017 was 27.91 ppb, which is significantly higher than those in 2015 and 2016 at 17.93 ppb and 16.55 ppb, respectively. During the 25-50 concentration percentile period of the $NH_3$, there was a WS of approximately 2 m/s east of the observation site, and during the 50-75 concentration percentile period, there was an obvious source northwest of the observation site, with a WS of approximately 4 m/s. During the 75-100 concentration percentile periods, the pollution sources were mainly local. This shows that in 2017, in addition to the pollution sources being distributed in the east and southeast, the higher $NH_3$ emissions were also contributed by the surrounding emission sources northwest of Chengdu.

**3.5.2 Gaseous precursors of NSA regional transport**

The PSCF is used to analyse the potential source distribution of pollutants to determine the regional transport characteristics of pollutants (Ji et al., 2019). Fig. 9 shows the PSCF analysis of NOx, $SO_2$ and $NH_3$, with significant differences in their potential

https://doi.org/10.5194/acp-2019-1142
Preprint. Discussion started: 26 February 2020


Atmospheric Chemistry and Physics Discussions

source distributions. The higher PSCF value of NOx was mainly distributed within 300 km west and southwest of Chengdu in 2015 (Ya'an, Meishan, Leshan and western Chengdu), north and south of Chengdu in 2016 (Deyang, Meishan, Leshan and northwestern Chengdu), and south and northeast of Chengdu in 2017 (Deyang, Mianyang, Meishan, Leshan and western Chengdu). Chengdu is located along the western margin of the Sichuan Basin. It was also observed through satellite remote sensing data that the higher $NO_2$ emissions in the Sichuan Basin are distributed in Chengdu and Chongqing (Fig. S16). As shown in Fig. 9, the higher PSCF values were concentrated in the surrounding areas of Chengdu, indicating that the Chengdu NOx was mainly from local emissions. The $SO_2$ emissions were widely distributed, mainly in the Sichuan Basin. Among them, Leshan city and Meishan city south of Chengdu have higher $SO_2$ emissions, and another higher emission source was distributed in Chongqing (Fig. S16). The PSCF analysis of $SO_2$ shows that the higher PSCF values were distributed in the western, southern and southwestern parts of Chengdu, and the western, southern and southwestern marginal regions of the Sichuan Basin were also important potential distribution areas. Therefore, comparison Figs. 9 and S16 shows that the main source of $SO_2$ may be distributed in the western, southern and southwestern edge areas of the Sichuan Basin. In particular, Leshan, Ya'an and Meishan were important potential sources. There were different sources of $NH_3$ emissions from 2015 to 2017, mainly distributed in the Sichuan Province. In 2015, the potential sources were mainly west of the Sichuan Basin, southwest of Chengdu city, which is approximately 100 km away from an important source. A higher PSCF was mainly distributed in Ya'an, Leshan, Meishan and Yibin in 2016. In 2017, the higher PSCF was mainly distributed in the western and northern areas of the Sichuan Basin, as well as Meishan and Leshan, which were close to Chengdu and contributed significantly. Northwest of Chengdu, Deyang, Mianyang and Guangyuan were important potential sources, and a small part also comes from south of Gansu and Shaanxi. Fig. S17 shows the Multiresolution Emission Inventory for China (MEIC) Gridded emissions of $NH_3$

https://doi.org/10.5194/acp-2019-1142
Preprint. Discussion started: 26 February 2020


Atmospheric Chemistry and Physics Discussions

628 in 2016 (Zhang et al., 2019). The higher $NH_3$ emissions were mainly concentrated in
629 the interior of the Sichuan Basin, especially near Chengdu, the western edge of the
630 basin. In comparison with Figs. 9 and S17, the regions with potential impacts on $NH_3$
631 concentration in Chengdu were mainly distributed in the Sichuan Basin, especially
632 south and northeast of Chengdu.

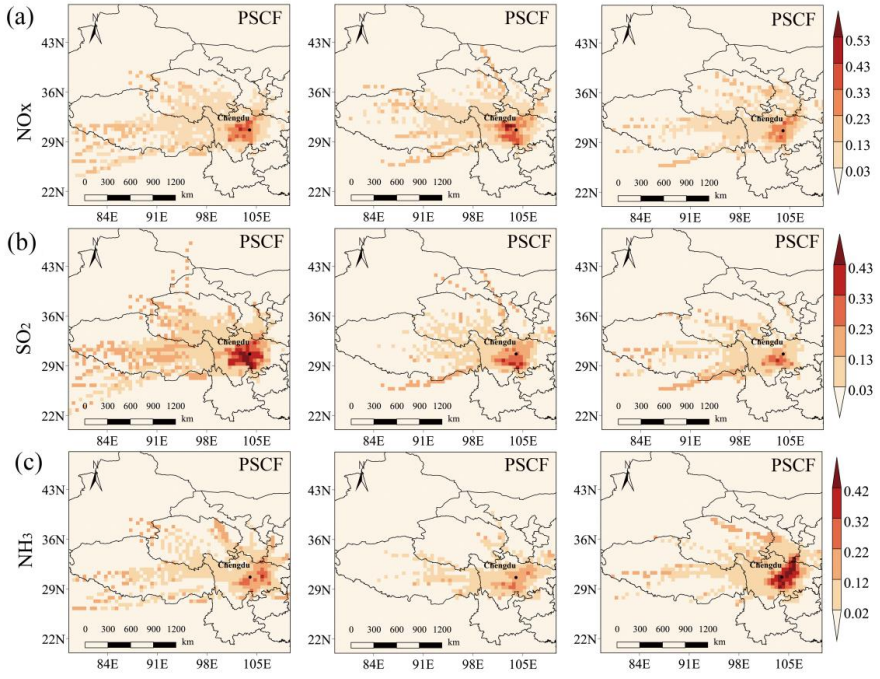


633

634 Fig. 9. PSCF of NOx, $SO_2$ and $NH_3$ (ppb) in Chengdu from 2015 to 2017.

635 **4 Conclusions**

636 The long-term observation experiment with hourly resolution of NSA from January 1,
637 2015 to December 31, 2017 was carried out in Chengdu in southwest China, which is
638 in the Sichuan Basin. The pollution characteristics of NSA's annual, monthly, seasonal,
639 diurnal and weekly variations were demonstrated. The characteristics of chemical
640 conversion, the relationship with carbonaceous aerosols, and the sensitivity of emission
641 reduction control were analysed. Finally, combined with meteorological factors and
642 PSCF simulation, the local emission and regional transport characteristics of NSA

https://doi.org/10.5194/acp-2019-1142
Preprint. Discussion started: 26 February 2020


Atmospheric Chemistry and Physics Discussions

643 gaseous precursors were also illustrated. The main conclusions were as follows:
644 (1) Compared with 2015, the concentration of $NO_3^-$ in 2017 did not decrease
645 significantly, while the concentrations of $SO_4^{2-}$ and $NH_4^+$ decreased. With the increase
646 in $PM_{2.5}$ concentration, the NSA mass concentration increased, accounting for 31.45-
647 37.78% of $PM_{2.5}$, but there was a downward trend, indicating that the contribution of
648 other unknown components to $PM_{2.5}$ may significantly increase with the aggravation of
649 pollution. Higher and lower NSA concentrations were seen in winter and summer,
650 respectively, and higher concentrations were seen more during the day than at night.
651 Although the NSA concentration on weekdays was slightly higher than that on
652 weekends, the mean difference between them was nonsignificant.
653 (2) With the increase in $PM_{2.5}$ concentration, aqueous phase oxidation was an important
654 process of NSA chemical conversion. The ammonia-rich environment in Chengdu
655 became increasingly obvious. Under this condition, the main strategy to reduce the
656 concentration of NSA was to continue to promote sulfate reduction and to strengthen
657 the control of nitrate and ammonium reductions. When controlling the decrease in
658 sulfate and nitrate, the decrease in ammonium will be obvious. NSA synergistic
659 emissions reduction control implementation can achieve a better emission reduction
660 effect. Regulation of the emission reduction ratio of NSA and reduction of the impact
661 on aerosol pH was also a problem worth further consideration.
662 (3) Local emissions and regional transport of NSA gaseous precursors have an
663 important impact on air pollution in Chengdu. In particular, NOx was the most obvious
664 contribution from the western, southern and southwestern margins of the Sichuan Basin
665 and local emissions in Chengdu. Northeast and west of Chengdu, there were high local
666 $SO_2$ emission sources, and combined with satellite remote sensing data and PSCF
667 analyses, within the Sichuan Basin, the cities of Leshan and Meishan south of Chengdu
668 may be important sources of $SO_2$ regional transport. The potential sources of $NH_3$ were
669 widely distributed, and the internal emissions of the Sichuan Basin may be important
670 potential contribution sources. Southwest, south and southeast of Chengdu, the

https://doi.org/10.5194/acp-2019-1142
Preprint. Discussion started: 26 February 2020


Atmospheric Chemistry and Physics Discussions

contribution was obvious. The analysis of local emissions and regional transport shows that implementing regional joint prevention, controlling emissions reduction working mechanisms and simultaneously promoting pollutant emission control are important implementation plans.

**Acknowledgements**

This work was supported by the People's Republic of China Science and Technology Department (No. 2018YFC0214001 and No. 2016YFC0202000) and the National Natural Science Foundation of China (No. 91544221).

**Data availability**

The data are available on request to the corresponding author.

**Author contribution**

XL, QT and LK designed and led this study. QT and MF was responsible for the observations. LK, MF, YL, YZ, CZ, CL analyzed the data. LK, YQ, JA, NC, YD, RZ and ZW discussed the results. LK and XL wrote the paper. All authors commented on the paper.

**Competing interests**

The authors declare that they have no conflict of interest.

**References**

An, Z., Huang, R. J., Zhang, R., Tie, X., Li, G., Cao, J., Zhou, W., Shi, Z., Han, Y., Gu, Z., and Ji, Y.: Severe haze in northern China: A synergy of anthropogenic emissions and atmospheric processes, Proceedings of the National Academy of Sciences of the United States of America, 116, 8657-8666, 10.1073/pnas.1900125116, 2019.

Ansari, A. S., and Pandis, S. N.: The effect of metastable equilibrium states on the partitioning of nitrate between the gas and aerosol phases, Atmospheric Environment, 34, 157-168, 10.1016/s1352-2310(99)00242-3, 2000.

Beijing Municipal Ecology and Environment Bureau: Beijing Environmental Statement. http://sthjj.beijing.gov.cn/bjhrb/xxgk/ywdt/hjzlzk/hjzkgb65/index.html，2017

Cao, J., Lee, S.., Zhang, X., Chow, J., An, Z., Ho, K., Watson, J., Fung, K., Wang, Y., and Shen, Z.: Characterization of airborne carbonate over a site near Asian dust source regions during spring 2002 and its climatic and environmental significance, Journal of Geophysical Research-Atmospheres, 110, 10.1029/2004jd005244, 2005.

https://doi.org/10.5194/acp-2019-1142
Preprint. Discussion started: 26 February 2020


Atmospheric Chemistry and Physics Discussions

704 Chang, X., Wang, S., Zhao, B., Cai, S., and Hao, J.: Assessment of inter-city transport
705 of particulate matter in the Beijing-Tianjin-Hebei region, Atmospheric
706 Chemistry and Physics, 18, 4843-4858, 10.5194/acp-18-4843-2018, 2018.
707 Chen, L., Zhu, J., Liao, H., Gao, Y., Qiu, Y., Zhang, M., Liu, Z., Li, N., and Wang, Y.:
708 Assessing the formation and evolution mechanisms of severe haze pollution in
709 the Beijing–Tianjin–Hebei region using process analysis, Atmospheric
710 Chemistry and Physics, 19, 10845-10864, 10.5194/acp-19-10845-2019, 2019a.
711 Chen, Z., Chen, D., Wen, W., Zhuang, Y., Kwan, M., Chen, B., Zhao, B., Yang, L., Gao,
712 B., Li, R., and Xu, B.: Evaluating the "2+26" regional strategy for air quality
713 improvement during two air pollution alerts in Beijing: variations in $PM_{2.5}$
714 concentrations, source apportionment, and the relative contribution of local
715 emission and regional transport, Atmospheric Chemistry and Physics, 19, 6879-
716 6891, 10.5194/acp-19-6879-2019, 2019b.
717 Chengdu Municipal Ecology and Environment Bureau: Ambient air quality report.
718 http://sthj.chengdu.gov.cn/cdhbj/c110802/list_1.shtml, 2017.
719 Cheng, J., Su, J., Cui, T., Li, X., Dong, X., Sun, F., Yang, Y., Tong, D., Zheng, Y., Li,
720 Y., Li, J., Zhang, Q., and He, K.: Dominant role of emission reduction in PM2.5
721 air quality improvement in Beijing during 2013–2017: a model-based
722 decomposition analysis, Atmospheric Chemistry and Physics, 19, 6125-6146,
723 10.5194/acp-19-6125-2019, 2019.
724 Cheng, Y., Zheng, G., Wei, C., Mu, Q., Zheng, B., Wang, Z., Gao, M., Zhang, Q., He,
725 K., Carmichael, G., Poschl, U., and Su, H.: Reactive nitrogen chemistry in
726 aerosol water as a source of sulfate during haze events in China, Science
727 Advances, 2, 10.1126/sciadv.1601530, 2016.
728 the Sate Council: Three-Year Action Plan for Winning the Blue Sky Defense Battle.
729 http://www.gov.cn/zhengce/content/2018-07/03/content_5303158.htm, 2018.
730 Ding, J., Zhao, P., Su, J., Dong, Q., Du, X., and Zhang, Y.: Aerosol pH and its driving
731 factors in Beijing, Atmospheric Chemistry and Physics, 19, 7939-7954,
732 10.5194/acp-19-7939-2019, 2019.
733 Fountoukis, C., and Nenes, A.: ISORROPIA II: a computationally efficient
734 thermodynamic equilibrium model for $K^+$-$Ca^{2+}$-$Mg^{2+}$-$NH_4^+$-$Na^+$-$SO_4^{2-}$-$NO_3^-$-
735 $Cl^-$-$H_2O$ aerosols, Atmospheric Chemistry and Physics, 7, 4639-4659,
736 10.5194/acp-7-4639-2007, 2007.
737 Fountoukis, C., Nenes, A., Sullivan, A., Weber, R., Van Reken, T., Fischer, M., Matias,
738 E., Moya, M., Farmer, D., and Cohen, R.: Thermodynamic characterization of
739 Mexico City aerosol during MILAGRO 2006, Atmospheric Chemistry and
740 Physics, 9, 2141-2156, 10.5194/acp-9-2141-2009, 2009.
741 Fu, G., Xu, W., Yang, R.., Li, J., and Zhao, C.: The distribution and trends of fog and
742 haze in the North China Plain over the past 30 years, Atmospheric Chemistry
743 and Physics, 14, 11949-11958, 10.5194/acp-14-11949-2014, 2014.
744 Gui, K., Che, H., Wang, Y., Wang, H., Zhang, L., Zhao, H., Zheng, Y., Sun, T., and
745 Zhang, X.: Satellite-derived PM2.5 concentration trends over Eastern China

https://doi.org/10.5194/acp-2019-1142
Preprint. Discussion started: 26 February 2020




from 1998 to 2016: Relationships to emissions and meteorological parameters, Environmental pollution, 247, 1125-1133, 10.1016/j.envpol.2019.01.056, 2019.

Guo, H., Liu, J., Froyd, K. D., Roberts, J. M., Veres, P. R., Hayes, P. L., Jimenez, J. L., Nenes, A., and Weber, R. J.: Fine particle pH and gas-particle phase partitioning of inorganic species in Pasadena, California, during the 2010 CalNex campaign, Atmospheric Chemistry and Physics, 17, 5703-5719, 10.5194/acp-17-5703-2017, 2017.

Ministry of Ecology and Environment of the People's Republic of China: Detailed regulations for the implementation of air pollution control action plan in Beijing, Tianjin, Hebei and surrounding areas. http://www.mee.gov.cn/gkml/hbb/bwj/201309/t20130918_260414.htm, 2013.

Guo, S., Hu, M., Zamora, M., Peng, J., Shang, D., Zheng, J., Du, Z., Wu, Z., Shao, M., Zeng, L., Molina, M., and Zhang, R.: Elucidating severe urban haze formation in China, Proceedings of the National Academy of Sciences of the United States of America, 111, 17373-17378, 10.1073/pnas.1419604111, 2014.

He, H., Wang, Y., Ma, Q., Ma, J., Chu, B., Ji, D., Tang, G., Liu, C., Zhang, H., and Hao, J.: Mineral dust and NOx promote the conversion of $SO_2$ to sulfate in heavy pollution days, Scientific reports, 4, 4172, 2014.

Ji, D., Yan, Y., Wang, Z., He, J., Liu, B., Sun, Y., Gao, M., Li, Y., Cao, W., Cui, Y., Hu, B., Xin, J., Wang, L., Liu, Z., Tang, G., and Wang, Y.: Two-year continuous measurements of carbonaceous aerosols in urban Beijing, China: Temporal variations, characteristics and source analyses, Chemosphere, 200, 191-200, 10.1016/j.chemosphere.2018.02.067, 2018.

Ji, D., Gao, W., Maenhaut, W., He, J., Wang, Z., Li, J., Du, W., Wang, L., Sun, Y., Xin, J., Hu, B., and Wang, Y.: Impact of air pollution control measures and regional transport on carbonaceous aerosols in fine particulate matter in urban Beijing, China: insights gained from long-term measurement, Atmospheric Chemistry and Physics, 19, 8569-8590, 10.5194/acp-19-8569-2019, 2019.

Kong, L., Hu, M., Tan, Q., Feng, M., Qu, Y., An, J., Zhang, Y., Liu, X., Cheng, N., Deng, Y., Zhai, R., and Wang, Z.: Key role of atmospheric water content in the formation of regional haze in southern China, Atmospheric Environment, 216, 10.1016/j.atmosenv.2019.116918, 2019.

Kong, L., Hu, M., Tan, Q., Feng, M., Qu, Y., An, J., Zhang, Y., Liu, X., and Cheng, N.: Aerosol optical properties under different pollution levels in the Pearl River Delta (PRD) region of China, Journal of environmental sciences, 87, 49-59, 10.1016/j.jes.2019.02.019, 2020.

Kopp, R. E., and Mauzerall, D. L.: Assessing the climatic benefits of black carbon mitigation, Proceedings of the National Academy of Sciences of the United States of America, 107, 11703-11708, 2010.

Li, H., Cheng, J., Zhang, Q., Zheng, B., Zhang, Y., Zheng, G., and He, K.: Rapid transition in winter aerosol composition in Beijing from 2014 to 2017: response to clean air actions, Atmospheric Chemistry and Physics, 19, 11485-11499,

https://doi.org/10.5194/acp-2019-1142
Preprint. Discussion started: 26 February 2020




10.5194/acp-19-11485-2019, 2019a.

Li, K., Jacob, D. J., Liao, H., Zhu, J., Shah, V., Shen, L., Bates, K. H., Zhang, Q., and Zhai, S.: A two-pollutant strategy for improving ozone and particulate air quality in China, Nature Geoscience, 10.1038/s41561-019-0464-x, 2019b.

Li, L., Tan, Q., Zhang, Y., Feng, M., Qu, Y., An, J., and Liu, X.: Characteristics and source apportionment of PM2.5 during persistent extreme haze events in Chengdu, southwest China, Environmental pollution, 230, 718-729, 10.1016/j.envpol.2017.07.029, 2017.

Li, M., Wang, T., Xie, M., Li, S., Zhuang, B., Huang, X., Chen, P., Zhao, M., and Liu, J.: Formation and Evolution Mechanisms for Two Extreme Haze Episodes in the Yangtze River Delta Region of China During Winter 2016, Journal of Geophysical Research: Atmospheres, 124, 3607-3623, 10.1029/2019jd030535, 2019c.

Li, Y., Ye, C., Liu, J., Zhu, Y., Wang, J., Tan, Z., Lin, W., Zeng, L., and Zhu, T.: Observation of regional air pollutant transport between the megacity Beijing and the North China Plain, Atmospheric Chemistry and Physics, 16, 14265-14283, 10.5194/acp-16-14265-2016, 2016.

Liu, K., Wu, Q., Wang, L., Wang, S., Liu, T., Ding, D., Tang, Y., Li, G., Tian, H., Duan, L., Wang, X., Fu, X., Feng, X., and Hao, J.: Measure-Specific Effectiveness of Air Pollution Control on China's Atmospheric Mercury Concentration and Deposition during 2013-2017, Environmental Science & Technology, 53, 8938-8946, 10.1021/acs.est.9b02428, 2019a.

Liu, L., Zhang, X., Wong, A. Y. H., Xu, W., Liu, X., Li, Y., Mi, H., Lu, X., Zhao, L., Wang, Z., Wu, X., and Wei, J.: Estimating global surface ammonia concentrations inferred from satellite retrievals, Atmospheric Chemistry and Physics, 19, 12051-12066, 10.5194/acp-19-12051-2019, 2019b.

Liu, M., Huang, X., Song, Y., Tang, J., Cao, J., Zhang, X., Zhang, Q., Wang, S., Xu, T., Kang, L., Cai, X., Zhang, H., Yang, F., Wang, H., Yu, J. Z., Lau, A. K. H., He, L., Huang, X., Duan, L., Ding, A., Xue, L., Gao, J., Liu, B., and Zhu, T.: Ammonia emission control in China would mitigate haze pollution and nitrogen deposition, but worsen acid rain, Proceedings of the National Academy of Sciences of the United States of America, 116, 7760-7765, 10.1073/pnas.1814880116, 2019c.

Liu, X., Zhang, Y., Cheng, Y., Hu, M., and Han, T.: Aerosol hygroscopicity and its impact on atmospheric visibility and radiative forcing in Guangzhou during the 2006 PRIDE-PRD campaign, Atmospheric Environment, 60, 59-67, 10.1016/j.atmosenv.2012.06.016, 2012.

Liu, X., Zhang, Y., Han, W., Tang, A., Shen, J., Cui, Z., Vitousek, P., Erisman, J. W., Goulding, K., Christie, P., Fangmeier, A., and Zhang, F.: Enhanced nitrogen deposition over China, Nature, 494, 459-462, 10.1038/nature11917, 2013a.

Liu, X. G., Li, J., Qu, Y., Han, T., Hou, L., Gu, J., Chen, C., Yang, Y., Yang, T., and Zhang, Y.: Formation and evolution mechanism of regional haze: A case study

https://doi.org/10.5194/acp-2019-1142
Preprint. Discussion started: 26 February 2020




in the megacity Beijing, China, Atmospheric Chemistry and Physics, 13, 4501-4514, 10.5194/acp-13-4501-2013, 2013b.

Liu, Y., Zheng, M., Yu, M., Cai, X., Du, H., Li, J., Zhou, T., Yan, C., Wang, X., Shi, Z., Harrison, R. M., Zhang, Q., and He, K.: High-time-resolution source apportionment of $PM_{2.5}$ in Beijing with multiple models, Atmospheric Chemistry and Physics, 19, 6595-6609, 10.5194/acp-19-6595-2019, 2019d.

Malm, W. C., and Hand, J. L.: An examination of the physical and optical properties of aerosols collected in the IMPROVE program, Atmospheric Environment, 41, 3407-3427, 10.1016/j.atmosenv.2006.12.012, 2007.

Martin, L. R., and Good, T. W.: Catalyzed oxidation of sulfur-dioxide in solution-the iron-manganese synergism, Atmospheric Environment Part a-General Topics, 25, 2395-2399, 10.1016/0960-1686(91)90113-l, 1991.

Meier, J., Wehner, B., Massling, A., Birmili, W., Nowak, A., Gnauk, T., Brueggemann, E., Herrmann, H., Min, H., and Wiedensohler, A.: Hygroscopic growth of urban aerosol particles in Beijing (China) during wintertime: a comparison of three experimental methods, Atmospheric Chemistry and Physics, 9, 6865-6880, 10.5194/acp-9-6865-2009, 2009.

National Aeronautics and Space Administration: Giovanni data. https://giovanni.gsfc.nasa.gov/giovanni/, 2019.

National Oceanic and Atmospheric Administration: HYSPLIT data. ftp://arlftp.arlhq.noaa.gov/pub/archives/gdas1, 2019.

Ohta, S., and Okita, T.: A chemical characterization of atmospheric aerosol in Sapporo, Atmospheric Environment Part A General Topics, 24, 815-822, 1990.

Pan, Y., Tian, S., Liu, D., Fang, Y., Zhu, X., Zhang, Q., Zheng, B., Michalski, G., and Wang, Y.: Fossil Fuel Combustion-Related Emissions Dominate Atmospheric Ammonia Sources during Severe Haze Episodes: Evidence from (15)N-Stable Isotope in Size-Resolved Aerosol Ammonium, Environ Sci Technol, 50, 8049-8056, 10.1021/acs.est.6b00634, 2016.

Qiao, X., Guo, H., Tang, Y., Wang, P., Deng, W., Zhao, X., Hu, J., Ying, Q., and Zhang, H.: Local and regional contributions to fine particulate matter in the 18 cities of Sichuan Basin, southwestern China, Atmospheric Chemistry and Physics, 19, 5791-5803, 10.5194/acp-19-5791-2019, 2019.

Qin, W., Zhang, Y., Chen, J., Yu, Q., Cheng, S., Li, W., Liu, X., and Tian, H.: Variation, sources and historical trend of black carbon in Beijing, China based on ground observation and MERRA-2 reanalysis data, Environmental pollution, 245, 853-863, 10.1016/j.envpol.2018.11.063, 2019.

Song, M., Tan, Q., Feng, M., Qu, Y., Liu, X., An, J., and Zhang, Y.: Source apportionment and secondary transformation of atmospheric non-methane hydrocarbons in Chengdu, southwest China, Journal of Geophysical Research: Atmospheres, 123, 9741–9763, 10.1029/2018JD028479,2018.

Sun, Y., Zhuang, G., Tang, A. A., Wang, Y., and An, Z.: Chemical characteristics of $PM_{2.5}$ and $PM_{10}$ in haze-fog episodes in Beijing, Environmental Science &

https://doi.org/10.5194/acp-2019-1142
Preprint. Discussion started: 26 February 2020




872 Technology, 40, 3148-3155, 10.1021/es051533g, 2006.
873 Sun, Y., Wang, Z., Fu, P., Jiang, Q., Yang, T., Li, J., and Ge, X.: The impact of relative
874 humidity on aerosol composition and evolution processes during wintertime in
875 Beijing, China, Atmospheric Environment, 77, 927-934,
876 10.1016/j.atmosenv.2013.06.019, 2013.
877 Sun, Y., Jiang, Q., Wang, Z., Fu, P., Li, J., Yang, T., and Yin, Y.: Investigation of the
878 sources and evolution processes of severe haze pollution in Beijing in January
879 2013, Journal of Geophysical Research: Atmospheres, 119, 4380-4398,
880 10.1002/2014jd021641, 2014.
881 Tao, J., Zhang, L., Cao, J., and Zhang, R.: A review of current knowledge concerning
882 PM<sub>2. 5</sub> chemical composition, aerosol optical
883 properties and their relationships across China, Atmospheric Chemistry and
884 Physics, 17, 9485-9518, 10.5194/acp-17-9485-2017, 2017.
885 the People's government of Chengdu: Action plan for air pollution control in Chengdu.
886 http://gk.chengdu.gov.cn/govInfoPub/detail.action?id=64348&tn=6, 2014.
887 Tian, Y., Xiao, Z., Wang, H., Xing, P., Liao, G., Huangfu, Y., Shi, G., Chen, K., Bi, X.,
888 and Feng, Y.: Influence of the sampling period and time resolution on the PM
889 source apportionment: Study based on the high time-resolution data and long-
890 term daily data, Atmospheric Environment, 165, 301-309,
891 10.1016/j.atmosenv.2017.07.003, 2017.
892 Tie, X., Wu, D., and Brasseur, G.: Lung cancer mortality and exposure to atmospheric
893 aerosol particles in Guangzhou, China, Atmospheric Environment, 43, 2375-
894 2377, 10.1016/j.atmosenv.2009.01.036, 2009.
895 Tie, X., Huang, R. J., Cao, J., Zhang, Q., Cheng, Y., Su, H., Chang, D., Poschl, U.,
896 Hoffmann, T., Dusek, U., Li, G., Worsnop, D. R., and O'Dowd, C. D.: Severe
897 Pollution in China Amplified by Atmospheric Moisture, Scientific reports, 7,
898 15760, 10.1038/s41598-017-15909-1, 2017.
899 Tong, D., Geng, G., Jiang, K., Cheng, J., Zheng, Y., Hong, C., Yan, L., Zhang, Y., Chen,
900 X., Bo, Y., Lei, Y., Zhang, Q., and He, K.: Energy and emission pathways
901 towards PM2.5 air quality attainment in the Beijing-Tianjin-Hebei region by
902 2030, The Science of the total environment, 692, 361-370,
903 10.1016/j.scitotenv.2019.07.218, 2019.
904 Uria-Tellaetxe, I., and Carslaw, D. C.: Conditional bivariate probability function for
905 source identification, Environmental Modelling & Software, 59, 1-9, 2014.
906 Wang, G., Zhang, R., Gomez, M. E., Yang, L., Levy, Z. M., Hu, M., Lin, Y., Peng, J.,
907 Guo, S., Meng, J., and Li, J.: Persistent sulfate formation from London Fog to
908 Chinese haze, Proceedings of the National Academy Ofences of the United
909 States of America, 48, 13630-13635, 10.1073/pnas.1616540113, 2016.
910 Wang, Q., Zhuang, G., Kan, H., Liu, T., Deng, C., Jian, X., Lin, Y., Guo, Z., Ying, C.,
911 and Fu, Q.: Probing the severe haze pollution in three typical regions of China:
912 Characteristics, sources and regional impacts, Atmospheric Environment, 120,
913 76-88, 10.1016/j.atmosenv.2015.08.076, 2015.

https://doi.org/10.5194/acp-2019-1142
Preprint. Discussion started: 26 February 2020


Atmospheric Chemistry and Physics Discussions

914 Wang, Y., Zhang, X., and Draxler, R. R.: TrajStat: GIS-based software that uses various
915 trajectory statistical analysis methods to identify potential sources from long-
916 term air pollution measurement data, Environmental Modelling & Software, 24,
917 938-939, 2009.
918 Wu, X., Wu, Y., Zhang, S., Liu, H., Fu, L., and Hao, J.: Assessment of vehicle emission
919 programs in China during 1998-2013: Achievement, challenges and
920 implications, Environmental pollution, 214, 556-567,
921 10.1016/j.envpol.2016.04.042, 2016.
922 Yang, Y., Liu, X., Qu, Y., Wang, J., An, J., Zhang, Y., and Zhang, F.: Formation
923 mechanism of continuous extreme haze episodes in the megacity Beijing, China,
924 in January 2013, Atmospheric Research, 155, 192-203,
925 10.1016/j.atmosres.2014.11.023, 2015a.
926 Yang, Y., Liu, X., Qu, Y., An, J., Jiang, R., Zhang, Y., Sun, Y., Wu, Z., Zhang, F., Xu,
927 W., and Ma, Q.: Characteristics and formation mechanism of continuous hazes
928 in China: a case study during the autumn of 2014 in the North China Plain,
929 Atmospheric Chemistry and Physics, 15, 8165-8178, 10.5194/acp-15-8165-
930 2015, 2015b.
931 Yao, L., Garmash, O., Bianchi, F., Zheng, J., Yan, C., Kontkanen, J., Junninen, H.,
932 Mazon, S. B., Ehn, M., Paasonen, P., Sipila, M., Wang, M., Wang, X., Xiao, S.,
933 Chen, H., Lu, Y., Zhang, B., Wang, D., Fu, Q., Geng, F., Li, L., Wang, H., Qiao,
934 L., Yang, X., Chen, J., Kerminen, V. M., Petaja, T., Worsnop, D. R., Kulmala,
935 M., and Wang, L.: Atmospheric new particle formation from sulfuric acid and
936 amines in a Chinese megacity, Science, 361, 278-281, 10.1126/science.aao4839,
937 2018.
938 Zhang, G., Li, J., Li, X., Xu, Y., Guo, L.-L., Tang, J., Lee, C., Liu, X., and Chen, Y.:
939 Impact of anthropogenic emissions and open biomass burning on regional
940 carbonaceous aerosols in South China, Environmental pollution, 158, 3392-
941 3400, 10.1016/j.envpol.2010.07036, 2010.
942 Zhang, H., Cheng, S., Li, J., Yao, S., and Wang, X.: Investigating the aerosol mass and
943 chemical components characteristics and feedback effects on the meteorological
944 factors in the Beijing-Tianjin-Hebei region, China, Environmental pollution,
945 244, 495-502, 10.1016/j.envpol.2018.10.087, 2019.
946 Zhang, R., Wang, G., Guo, S., Zamora, M. L., Ying, Q., Lin, Y., Wang, W., Hu, M., and
947 Wang, Y.: Formation of urban fine particulate matter, Chemical Reviews, 115,
948 3803-3855, 2015.
949 Zhang, Y., Chen, J., Yang, H., Li, R., and Yu, Q.: Seasonal variation and potential source
950 regions of $PM_{2.5}$-bound PAHs in the megacity Beijing, China: Impact of
951 regional transport, Environmental pollution, 231, 329-338,
952 10.1016/j.envpol.2017.08.025, 2017.
953 Zhao, B., Zheng, H., Wang, S., Smith, K. R., Lu, X., Aunan, K., Gu, Y., Wang, Y., Ding,
954 D., Xing, J., Fu, X., Yang, X., Liou, K.-N., and Hao, J.: Change in household
955 fuels dominates the decrease in $PM_{2.5}$ exposure and premature mortality in

https://doi.org/10.5194/acp-2019-1142
Preprint. Discussion started: 26 February 2020




China in 2005-2015, Proceedings of the National Academy of Sciences of the United States of America, 115, 12401-12406, 10.1073/pnas.1812955115, 2018.

Zhao, H., Li, X., Zhang, Q., Jiang, X., Lin, J., Peters, G. G., Li, M., Geng, G., Zheng, B., Huo, H., Zhang, L., Wang, H., Davis, S. J., and He, K.: Effects of atmospheric transport and trade on air pollution mortality in China, Atmospheric Chemistry and Physics, 17, 10367-10381, 10.5194/acp-17-10367-2017, 2017.

Zheng, G., Duan, F., Ma, Y., Zhang, Q., Huang, T., Kimoto, T., Cheng, Y., Su, H., and He, K.: Episode-Based Evolution Pattern Analysis of Haze Pollution: Method Development and Results from Beijing, China, Environ Sci Technol, 50, 4632-4641, 10.1021/acs.est.5b05593, 2016.

Zheng, H., Kong, S., Yan, Q., Wu, F., Cheng, Y., Zheng, S., Wu, J., Yang, G., Zheng, M., Tang, L., Yin, Y., Chen, K., Zhao, T., Liu, D., Li, S., Qi, S., Zhao, D., Zhang, T., Ruan, J., and Huang, M.: The impacts of pollution control measures on $PM_{2.5}$ reduction: Insights of chemical composition, source variation and health risk, Atmospheric Environment, 197, 103-117, 10.1016/j.atmosenv.2018.10.023, 2019.

Zhong, J., Zhang, X., Wang, Y., Wang, J., Shen, X., Zhang, H., Wang, T., Xie, Z., Liu, C., Zhang, H., Zhao, T., Sun, J., Fan, S., Gao, Z., Li, Y., and Wang, L.: The two-way feedback mechanism between unfavorable meteorological conditions and cumulative aerosol pollution in various haze regions of China, Atmospheric Chemistry and Physics, 19, 3287-3306, 10.5194/acp-19-3287-2019, 2019.

Zhu, J., Chen, L., Liao, H., and Dang, R.: Correlations between $PM_{2.5}$ and Ozone over China and Associated Underlying Reasons, Atmosphere, 10, 10.3390/atmos10070352, 2019.

Zhang, Q., Streets, D. G., Carmichael, G. R., He, K. B., Huo, H., Kannari, A., Klimont, Z., Park, I. S., Reddy, S., Fu, J. S., Chen, D., Duan, L., Lei, Y., Wang, L. T., and Yao, Z. L.: Asian emissions in 2006 for the NASA INTEX-B mission, Atmospheric Chemistry and Physics, 9, 5131-5153, 2009.